



*J. Serb. Chem. Soc.* 74 (12) 1401–1411 (2009)  
JSCS–3927

Journal of  
the Serbian  
Chemical Society

JSCS@tmf.bg.ac.rs • www.shd.org.rs/JSCS

UDC 546.87'824+546.832–31+546.831–  
31:537.31:621.352

Original scientific paper

## Mechanochemical synthesis and electrical conductivity of nanocrystalline $\delta$ -Bi<sub>2</sub>O<sub>3</sub> stabilized by HfO<sub>2</sub> and ZrO<sub>2</sub>

MIODRAG ZDUJIĆ<sup>1\*#</sup>, DEJAN POLETI<sup>2#</sup>, ČEDOMIR JOVALEKIĆ<sup>3</sup>  
and LJILJANA KARANOVIC<sup>4</sup>

<sup>1</sup>*Institute of Technical Sciences of the Serbian Academy of Science and Arts, Knez Mihailova 35, 11000 Belgrade,* <sup>2</sup>*Department of General and Inorganic Chemistry, Faculty of Technology and Metallurgy, University of Belgrade, Karnegijeva 4, 11000 Belgrade,* <sup>3</sup>*Institute for Multidisciplinary Research, Kneza Višeslava 1a, 11000 Belgrade and* <sup>4</sup>*Laboratory of Crystallography, Faculty of Mining and Geology, University of Belgrade, Dušina 7, 11000 Belgrade, Serbia*

(Received 13 May, revised 22 June 2009)

**Abstract:** A powder mixture of  $\alpha$ -Bi<sub>2</sub>O<sub>3</sub> and HfO<sub>2</sub>, in the molar ratio 2:3, was mechanochemically treated in a planetary ball mill under air, using zirconium oxide vials and balls as the milling medium. After 50 h of milling, the mechanochemical reaction led to the formation of a nanocrystalline  $\delta$ -Bi<sub>2</sub>O<sub>3</sub> phase (fluorite-type solid solution Bi<sub>0.78</sub>Hf<sub>0.59</sub>Zr<sub>0.63</sub>O<sub>3.61</sub>), with a crystallite size of 20 nm. The mechanochemical reaction started at a very beginning of milling accompanied by an accumulation of ZrO<sub>2</sub> arising from the milling tools. The samples prepared after various milling times were characterized by X-ray powder diffraction and DSC analysis. The electrical properties of the as-milled and pressed Bi<sub>0.78</sub>Hf<sub>0.59</sub>Zr<sub>0.63</sub>O<sub>3.61</sub> powder were studied using impedance spectroscopy in the temperature range from 100 to 700 °C under air. The electrical conductivity was determined to be  $9.43 \times 10^{-6}$  and 0.080 S cm<sup>-1</sup> for the temperatures of 300 and 700 °C, respectively.

**Keywords:** bismuth(III) oxide; milling; X-ray diffraction; electrical conductivity; fuel cells.

### INTRODUCTION

In recent years, there has been considerable interest in the study of materials based on Bi<sub>2</sub>O<sub>3</sub> owing to their physical properties, such as ionic conductivity, ferroelectricity, photoconductivity and photoluminescence. The ferroelectric nature of some bismuth-rich compounds, e.g., Bi<sub>4</sub>Ti<sub>3</sub>O<sub>12</sub>, CaBi<sub>3</sub>Ti<sub>3</sub>O<sub>12-x</sub> and

\* Corresponding author. E-mail: [miodrag.zdujic@itn.sanu.ac.rs](mailto:miodrag.zdujic@itn.sanu.ac.rs)

# Serbian Chemical Society member.

doi: 10.2298/JSC0912401Z

SrBi<sub>2</sub>(Ta,Nb)<sub>2</sub>O<sub>9</sub>, make them important materials for the manufacture of ferroelectric random access memories,<sup>1</sup> while the  $\delta$ -Bi<sub>2</sub>O<sub>3</sub> polymorph, with a fluorite-type structure, has the highest oxide-ion conductivity of all known compounds,<sup>2</sup> providing useful properties for its application in solid oxide fuel cells and gas sensors.<sup>3,4</sup>

Bismuth(III) oxide, Bi<sub>2</sub>O<sub>3</sub>, is known to appear in five polymorphs, as the  $\alpha$ -,  $\beta$ -,  $\gamma$ -,  $\delta$ - and  $\varepsilon$ -phase.<sup>5-7</sup> The room-temperature monoclinic  $\alpha$ -Bi<sub>2</sub>O<sub>3</sub> transforms upon heating at 729 °C to the high-temperature cubic  $\delta$ -Bi<sub>2</sub>O<sub>3</sub>, which is stable up to the melting point at 825 °C.<sup>8</sup> Upon cooling, two metastable phases may occur depending on the applied thermal treatment, *i.e.*, the tetragonal  $\beta$ -phase near 650 °C and the body-centered cubic  $\gamma$ -phase near 640 °C. Usually these phases transform into the  $\alpha$ -phase on further cooling.<sup>5</sup>

The structure of the  $\delta$ -phase is based on a face-centered cubic cation sublattice and can be described as a defective fluorite structure where one quarter of the available anion sites are vacant.<sup>6,9</sup> The disorder of the oxide ions in the structure has been investigated in detail,<sup>10-12</sup> and it was found that a high concentration of oxygen vacancies, combined with the high polarizability of the Bi<sup>3+</sup> 6s<sup>2</sup> lone electron pairs, increases the oxide ion mobility in this compound.<sup>13</sup>

Pure  $\delta$ -Bi<sub>2</sub>O<sub>3</sub> cannot be quenched to room temperature.<sup>14</sup> Nevertheless, the stability of the  $\delta$ -Bi<sub>2</sub>O<sub>3</sub> phase at low temperatures can be achieved by substituting Bi<sup>3+</sup> with different mono to pentavalent cations.<sup>15-17</sup> However, the stability improvement is usually accompanied by a decrease in the ionic conductivity. Thus, the substitution of Bi<sup>3+</sup> by higher-valent cations, such as Ti<sup>4+</sup>, Zr<sup>4+</sup> and Hf<sup>4+</sup> should result in a reduction of the vacancy concentration.<sup>13</sup>

Knowing that mechanochemical treatment is a process producing metastable (amorphous, nanocrystalline, supersaturated solid solutions) materials, this technique has already been employed for the study of various Bi<sub>2</sub>O<sub>3</sub>-containing systems.<sup>18,19</sup> One of the recent studies showed that mechanochemical treatment applied to the 2Bi<sub>2</sub>O<sub>3</sub>·3ZrO<sub>2</sub> system led to the gradual formation of a nanocrystalline phase which resembles  $\delta$ -Bi<sub>2</sub>O<sub>3</sub>.<sup>20</sup> Following this line, it seemed quite reasonable to undertake an examination of the analogous 2Bi<sub>2</sub>O<sub>3</sub>·3HfO<sub>2</sub> system. However, after prolonged milling for 50 h, a significant amount of ZrO<sub>2</sub>, originating from the milling medium, accumulated in the system yielding a final sample with the formula Bi<sub>0.78</sub>Hf<sub>0.59</sub>Zr<sub>0.63</sub>O<sub>3.61</sub>. Herein, structural, thermal and electrical investigations of a hafnium/zirconium-substituted bismuth oxide that adopts a fluorite-type  $\delta$ -Bi<sub>2</sub>O<sub>3</sub> structure, a material with very promising electrical properties, are presented.

#### EXPERIMENTAL

A mixture of commercial Bi<sub>2</sub>O<sub>3</sub> (> 99 % purity) and HfO<sub>2</sub> (> 98.5 % purity) powders in a 2:3 molar ratio was used as the starting material. By the X-ray powder diffraction (XRPD) technique, the Bi<sub>2</sub>O<sub>3</sub> was identified as being in the stable  $\alpha$ -Bi<sub>2</sub>O<sub>3</sub>, bismite form (JCPDS card

41-1449), whereas the HfO<sub>2</sub> was in the monoclinic modification (JCPDS card 34-0104), but contained about 1.5 wt. % of ZrO<sub>2</sub>. Mechanochemical treatment was performed in a Fritsch Pulverisette 5 planetary ball mill. Zirconia vials of 500 cm<sup>3</sup> volume charged with 93 zirconia balls of a nominal diameter of 10 mm were used as the milling medium. The mass of the powder mixtures was 15 g, giving a ball-to-powder mass ratio of 20:1. The angular velocities of the supporting disc and vials was 33.2 (317) and 41.5 rad s<sup>-1</sup> (396 rpm), respectively. The mixtures were milled for 10 and 30 min, as well as for 1, 10, 20 and 50 h in an air atmosphere with no addition of lubricant (dry milling). Each milling run was realized with a fresh powder mixture and without opening the vials for the specified milling period.

The X-ray powder diffraction data were collected on a Rigaku PH 1050 diffractometer with Cu-K $\alpha$  graphite-monochromatized radiation ( $\lambda = 1.5418 \text{ \AA}$ ) in the  $2\theta$  range 10–80° (step-length: 0.02°  $2\theta$ , scan time: 5 s). The program PowderCell,<sup>21</sup> was used for an approximate phase analysis in a Rietveld-like refinement. Unit cell parameters were obtained by the least-squares method using the program LSUCRIPC.<sup>22</sup> The mean crystallite size,  $\langle D \rangle$ , of the sample milled for 50 h was calculated by the Scherrer formula.<sup>23</sup> The sample milled for 50 h was tested using the EDXR fluorescence technique, which confirmed the presence of Bi, Hf and Zr only. The composition of the sample was determined by EDAX and re-checked by ICP analysis. The mean Zr content was 15.2 wt. %, yielding the formula Bi<sub>0.78</sub>Hf<sub>0.59</sub>Zr<sub>0.63</sub>O<sub>3.61</sub>. The particle morphology of the prepared material can be seen in Fig. 1.

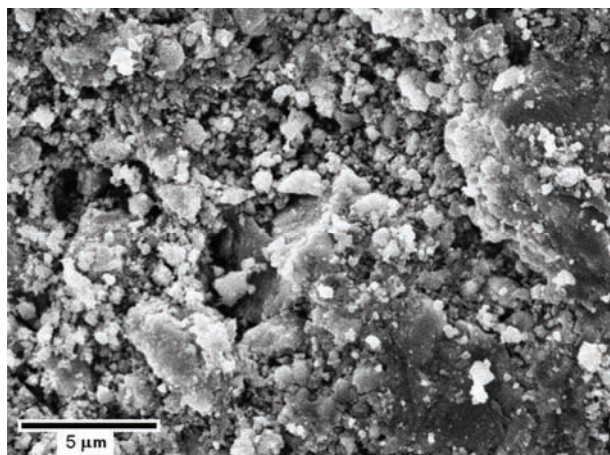


Fig. 1. SEM of the Bi<sub>0.78</sub>Hf<sub>0.59</sub>Zr<sub>0.63</sub>O<sub>3.61</sub> solid solution ( $\delta$ -Bi<sub>2</sub>O<sub>3</sub> phase) after 50 h of milling.

The thermal behavior of the initial mixture and powders milled for 1, 20 and 50 h was investigated from room temperature to 900 °C using an SDT Q600 simultaneous DSC–TGA instrument (TA Instruments) with a heating and cooling rate of 20 °C min<sup>-1</sup> under a dynamic (100 cm<sup>3</sup> min<sup>-1</sup>) N<sub>2</sub> atmosphere.

The electrodes for the electrical measurements were applied to polished disc surfaces (diameter 8 mm, thickness 1 mm) pressed under 1 MPa, by the screen printing method. The silver paste was polymerized at 200 °C for 30 min. AC impedance measurements were performed over the frequency range from 10<sup>-2</sup> to 3×10<sup>5</sup> Hz using a Gamry Potentiostat EIS 300. The amplitude of the input sine-wave signal was 10 mV. The ionic conductivity was measured up to 700 °C under an air atmosphere. The values of grain and grain boundary resistivity were

determined from the intersection of the semicircles with the  $Z'$  axis, while grain capacitance was calculated from the condition  $\omega RC = 1$ .

## RESULTS AND DISCUSSION

### Structural changes

As can be seen from Fig. 2, significant structural changes had already occurred after 10 min of milling. The XRPD pattern exhibits broad low intensity peaks, implying a very deformed and disordered structure. Both constituents mainly preserve their original monoclinic structure. In addition, some peaks may be assigned to  $\beta$ - $\text{Bi}_2\text{O}_3$  in an amount of about 15 wt. %, indicating that the mechanochemical reaction starts at the very beginning of milling. Such an early appearance of  $\beta$ - $\text{Bi}_2\text{O}_3$  is in accordance with the observed tendency for  $\text{ZrO}_2$  and  $\text{HfO}_2$  to stabilize this phase.<sup>24–26</sup>

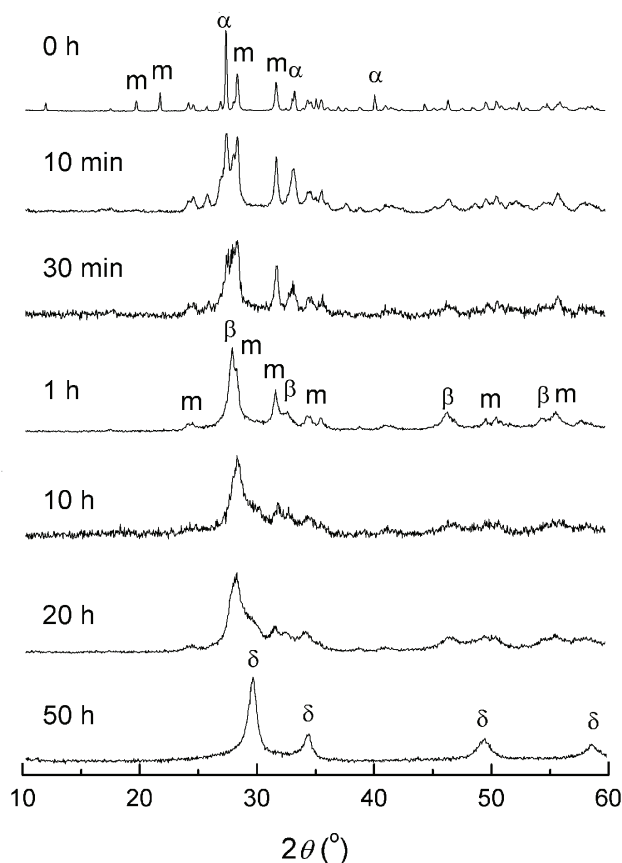


Fig. 2. XRPD Patterns of the powder mixtures after various milling times. Main maxima of the phases present are denoted as: m – monoclinic  $\text{HfO}_2$ ,  $\alpha$ ,  $\beta$  and  $\delta$  –  $\alpha$ - $\text{Bi}_2\text{O}_3$ ,  $\beta$ - $\text{Bi}_2\text{O}_3$  and  $\delta$ - $\text{Bi}_2\text{O}_3$ , respectively.

As milling continued, the formation of the  $\beta$ -Bi<sub>2</sub>O<sub>3</sub> phase progressed. Thus, the XRPD pattern of the sample milled for 30 min revealed that the strongest maxima of  $\alpha$ -Bi<sub>2</sub>O<sub>3</sub> (120 at 27.37° 2 $\theta$ ) and HfO<sub>2</sub> ( $\bar{1}11$  at 28.34° 2 $\theta$ ) merge into one broad peak at around 28° 2 $\theta$ . This peak is the most pronounced in the pattern of the sample milled for 1 h, and represents the main, (201) peak of the  $\beta$ -Bi<sub>2</sub>O<sub>3</sub> phase. After 1 h of milling, the approximate  $\beta$ -Bi<sub>2</sub>O<sub>3</sub> content was 50 wt. %.

Such a situation was maintained over a broad interval of mechanochemical treatment, so that differences in the patterns of samples milled for 10 and 20 h were hardly visible. Finally, in the XRPD pattern of the sample milled for 50 h, all peaks may be assigned to the  $\delta$ -Bi<sub>2</sub>O<sub>3</sub> phase. Therefore, mechanochemical treatment produced and stabilized the  $\delta$ -Bi<sub>2</sub>O<sub>3</sub> structure through the formation of a solid solution with HfO<sub>2</sub>, as well as with ZrO<sub>2</sub> introduced into the system as a consequence of vial and ball debris during prolonged milling. The obtained composition, *i.e.*, a solid solution of the formula Bi<sub>0.78</sub>Hf<sub>0.59</sub>Zr<sub>0.63</sub>O<sub>3.61</sub>, is in a nanocrystalline form with a crystallite size of about 20 nm. The microstructure of this sample (Fig. 1) is typical for milled ceramic materials showing small primary particles of about 0.1  $\mu$ m, as well as much larger aggregates of up to 10  $\mu$ m.

The high solubility of HfO<sub>2</sub> and ZrO<sub>2</sub> in Bi<sub>2</sub>O<sub>3</sub> can be explained by structural similarity of the high-temperature, cubic HfO<sub>2</sub>/ZrO<sub>2</sub> and  $\delta$ -Bi<sub>2</sub>O<sub>3</sub>. Cubic HfO<sub>2</sub> and ZrO<sub>2</sub> both have the fluorite structure (space group  $Fm\bar{3}m$ ) with  $a = 5.115(10)$  and  $5.065(10)$  Å, respectively.<sup>27</sup> In these phases, each cation is surrounded by eight equidistant oxygens. As already described in the Introduction,  $\delta$ -Bi<sub>2</sub>O<sub>3</sub> also has a fluorite-type structure, but with partially vacant oxide positions making space for the lone electron pair on Bi<sup>3+</sup>. High-temperature Hf<sub>1-x</sub>Bi<sub>x</sub>O<sub>2-x/2</sub> ( $x = 0.4-0.75$ ) and Zr<sub>1-x</sub>Bi<sub>x</sub>O<sub>2-x/2</sub> ( $x = 0.50-0.75$ ) phases with a defect fluorite structure have already been observed. At temperatures above 750 °C, both phases decompose giving different products.<sup>25</sup> The unit cell parameter of the present Bi<sub>0.78</sub>Hf<sub>0.59</sub>Zr<sub>0.63</sub>O<sub>3.61</sub> sample was  $a = 5.221(4)$  Å. This is between the values for HfO<sub>2</sub> and ZrO<sub>2</sub> unit cell parameters (see above) and the unit cell parameter of undoped  $\delta$ -Bi<sub>2</sub>O<sub>3</sub> (5.6549(9)–5.665(8) Å).<sup>6,10</sup>

#### Thermal behavior

The DSC examination of the powders milled for various milling times gave further understanding of the structures achieved with the progress of mechanochemical treatment. On heating, the starting powder mixture (before milling) exhibits two endothermic heat effects (Fig. 3a): the first is at about 740 °C (with an enthalpy change,  $\Delta H$ , of 30.5 J per gram of the powder mixture), which arises from the  $\alpha$ -Bi<sub>2</sub>O<sub>3</sub>  $\rightarrow$   $\delta$ -Bi<sub>2</sub>O<sub>3</sub> phase transition and the second at about 860 °C ( $\Delta H = 11.6$  J g<sup>-1</sup>) is assigned to the melting of  $\delta$ -Bi<sub>2</sub>O<sub>3</sub>.<sup>20</sup> Mechanochemical treatment for 1 h induced significant structural changes (Fig. 2), hence during heating, the temperature of the first heat effect was shifted to a lower temperature

of about 713 °C ( $\Delta H = 22.5 \text{ J g}^{-1}$ ), while during cooling, the  $\delta\text{-Bi}_2\text{O}_3$  transformed to the  $\beta$ -phase at about 576 °C ( $\Delta H = 20.7 \text{ J g}^{-1}$ ) (Fig. 3b). The fact that the sample milled for 1 h consisted of  $\beta\text{-Bi}_2\text{O}_3$  and  $\text{HfO}_2$ , as revealed by XRPD analysis, implies that first heat effect should be attributed to the  $\beta \rightarrow \delta$  phase transition.

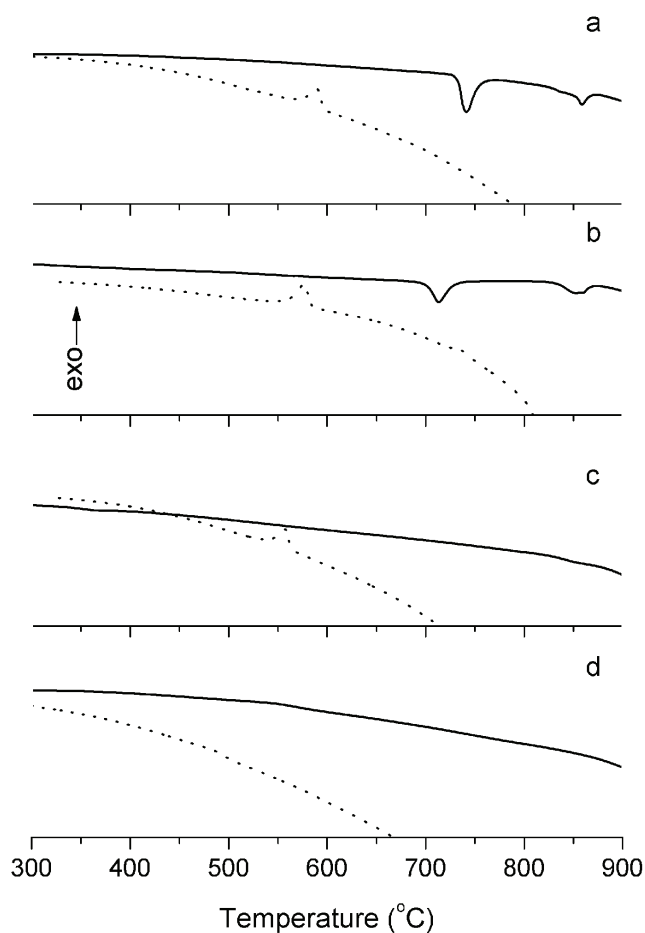


Fig. 3. DSC Curves (full line – heating, dotted line – cooling) of the powder mixtures: before (a) and after mechanochemical treatment for 1 (b), 20 (c), and 50 h (d).

Milling up to 20 h gradually deformed and mixed the constituents on the atomic level, and the powder milled for 20 h was stable during heating up to 900 °C, *i.e.*, no significant heat effect could be resolved on the DSC curve (Fig. 3c). However, on cooling, the  $\delta \rightarrow \beta$  phase transition occurred at about 556 °C ( $\Delta H = 16.7 \text{ J g}^{-1}$ ). Prolonged milling for 50 h, further refined and stabilized the structure, hence no recognizable heat effects may be detected during either heating or

cooling. This finding confirms that a single  $\delta$ -Bi<sub>2</sub>O<sub>3</sub> phase had been obtained, in agreement with the XRPD analysis. A similar thermal behavior was observed for the Bi<sub>0.85</sub>Eu<sub>0.1</sub>V<sub>0.05</sub>O<sub>1.55</sub> compound with a fluorite-type  $\delta$ -Bi<sub>2</sub>O<sub>3</sub> structure.<sup>15</sup>

#### Electrical measurements

Impedance spectroscopy was used to determine the electrical properties of the material mechanochemically synthesized for 50 h of milling. For such measurements, compacts were prepared by pressing only. No heat treatment was applied in order to preserve the structure attained after 50 h of milling, *i.e.*, to avoid possible phase transitions of  $\delta$ -Bi<sub>2</sub>O<sub>3</sub>, which could occur at higher temperatures. The density of the pressed samples was about 65 % of the theoretical density ( $\rho_x = 8.94 \text{ g cm}^{-3}$ ). Therefore, a high porosity plausibly implies considerably higher impedance values than if fully dense samples were used for the measurements. Moreover, the mechanochemical treatment created highly activated powders, which during pressing may form specific intergranular layers influencing, especially at low temperatures, the electrical characteristics.

Selected impedance spectra recorded in the temperature interval from 100 to 700 °C and in the frequency range from 300 kHz to 0.01 Hz are shown in Fig. 4. As can be seen, the curves are somewhat flattened, which may indicate deviation

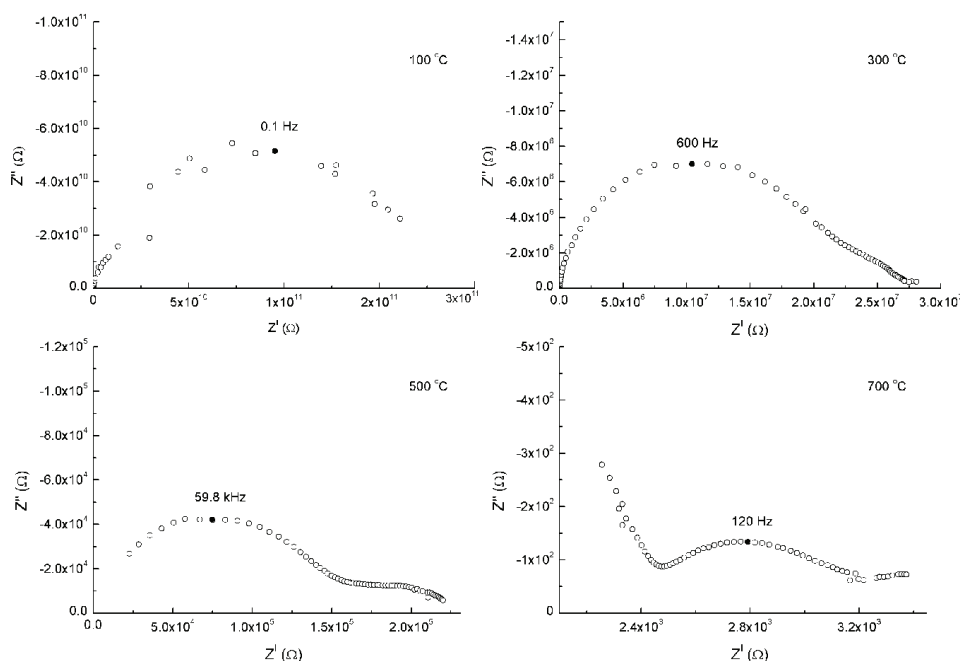


Fig. 4. Selected complex impedance plots measured at different temperatures of the Bi<sub>0.78</sub>Hf<sub>0.59</sub>Zr<sub>0.63</sub>O<sub>3.61</sub> solid solution ( $\delta$ -Bi<sub>2</sub>O<sub>3</sub> phase) powder prepared by mechanochemical treatment for 50 h, and compacted by pressing.

from Debye character of the samples.<sup>28</sup> With increasing temperature from 400 to 700 °C, the resistivity of the sample-to-electrode contact had a greater influence on the overall sample resistivity. This was most obvious at 700 °C, where the semicircle arising from the resistivity of the bulk sample material at higher frequency significantly declines.

It should be emphasized that no detectable structural changes were observed by XRPD analysis of the samples after the impedance–temperature measurements. This observation showed that prolonged heating does not cause any phase transition up to at least 700 °C, *i.e.*, the prepared  $\delta$ -Bi<sub>2</sub>O<sub>3</sub> samples were stable under these conditions. On the other hand, after a heat treatment (attempting to increase the density of the samples) at 820 °C for 24 h followed by slow (furnace) cooling or quenching, such metastable solid solutions transform into complex mixtures of either  $\delta$ -Bi<sub>2</sub>O<sub>3</sub>,  $\gamma$ -Bi<sub>2</sub>O<sub>3</sub> and monoclinic HfO<sub>2</sub>/ZrO<sub>2</sub> or  $\delta$ -Bi<sub>2</sub>O<sub>3</sub>,  $\beta$ -Bi<sub>2</sub>O<sub>3</sub> and monoclinic HfO<sub>2</sub>/ZrO<sub>2</sub>, respectively. (Monoclinic HfO<sub>2</sub> and ZrO<sub>2</sub> are indistinguishable by XRPD analysis because of their very similar unit cell parameters.)

The bulk resistivity is equal to the sum of the grain,  $R_g$ , and grain boundary,  $R_{gb}$ , resistivities. The specific resistivity,  $\rho$ , for various temperatures was calculated from the total resistivity, and the specific conductivity,  $\sigma = 1/\rho$ , as a function

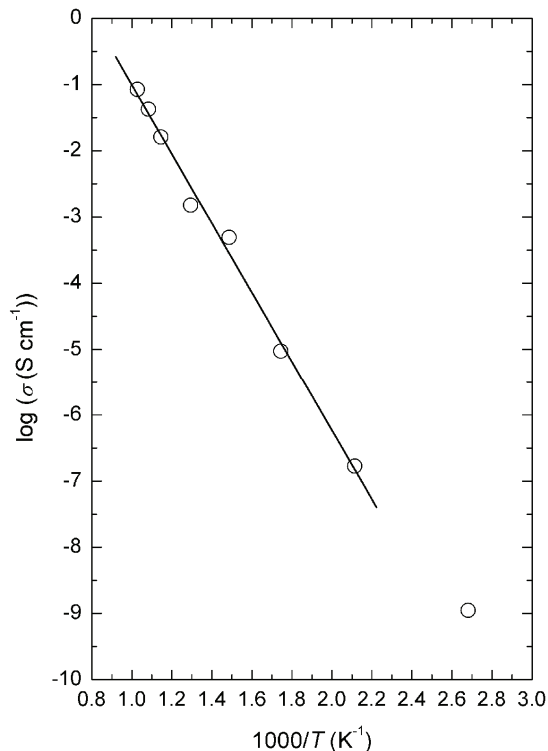


Fig. 5. Arrhenius plot of the  $\delta$ -Bi<sub>2</sub>O<sub>3</sub> (Bi<sub>0.78</sub>Hf<sub>0.59</sub>Zr<sub>0.63</sub>O<sub>3.61</sub>) powder prepared by mechanochemical treatment for 50 h, and compacted by pressing.



of  $1000/T$  is presented in Fig. 5. The obtained values of the electrical conductivity are  $\sigma_{300} = 9.43 \times 10^{-6}$  and  $\sigma_{700} = 0.080$  S cm<sup>-1</sup> for the temperatures 300 and 700 °C, respectively (Table I). In comparison with some Bi-containing phases, the conductivity of Bi<sub>0.78</sub>Hf<sub>0.59</sub>Zr<sub>0.63</sub>O<sub>3.61</sub> was lower than the electrical conductivity of pure  $\delta$ -Bi<sub>2</sub>O<sub>3</sub> ( $\sigma_{\text{bulk}} = 1$  S cm<sup>-1</sup> at 730 °C),<sup>4</sup> and those of some Bi<sub>3</sub>Nb<sub>1-x</sub>Zr<sub>x</sub>O<sub>7-x/2</sub> compounds ( $\sigma_{600} = 0.114$  and  $0.123$  S cm<sup>-1</sup> for  $x = 0.80$  and  $0.90$ , respectively),<sup>16</sup> as well as of some compositions in the of Bi<sub>2</sub>O<sub>3</sub>-Er<sub>2</sub>O<sub>3</sub>-PbO system ( $\sigma_{750} = 0.49$  and  $0.72$  S cm<sup>-1</sup> for (BiO<sub>1.5</sub>)<sub>0.80</sub>(ErO<sub>1.5</sub>)<sub>0.11</sub>(PbO)<sub>0.09</sub> and (BiO<sub>1.5</sub>)<sub>0.85</sub>(ErO<sub>1.5</sub>)<sub>0.12</sub>(PbO)<sub>0.03</sub>, respectively).<sup>29</sup> Moreover, it is comparable with that for the Bi<sub>23</sub>V<sub>4</sub>O<sub>44.5</sub> compound ( $\sigma_{600} = 10^{-2}$  S cm<sup>-1</sup>),<sup>30</sup> or even higher in comparison to some other systems. For example, the electrical conductivities at 800 °C of the isostructural SrBi<sub>6</sub>V<sub>2</sub>O<sub>15</sub> and PbBi<sub>6</sub>V<sub>2</sub>O<sub>15</sub> are  $1.96 \times 10^{-3}$  and  $1.72 \times 10^{-3}$  S cm<sup>-1</sup>, respectively,<sup>31</sup> while for the Bi<sub>9</sub>SO<sub>16.5</sub> compound, conductivities from  $\approx 10^{-3}$  to  $\approx 10^{-2}$  S cm<sup>-1</sup> were found at 600 and 700 °C.<sup>32</sup> In addition,  $\sigma_{690} = 3.41 \times 10^{-2}$  S cm<sup>-1</sup> was obtained for the Pb<sub>2</sub>BiVO<sub>6</sub> compound.<sup>33</sup>

For the temperature range 200–700 °C, the calculated value of the activation energy,  $E_a = 1.03$  eV, was higher than the values for some other bismuth oxide compounds with similar grain sizes, for example,  $E_a = 0.7$  eV, for Bi<sub>4</sub>Ti<sub>3</sub>O<sub>12</sub>,<sup>34</sup> and  $E_a \approx 0.78$  eV for Bi<sub>23</sub>V<sub>4</sub>O<sub>44.5</sub>.<sup>30</sup>

As can be seen from Table I, the grain resistivity change with temperature is not so pronounced as it for the grain boundary resistivity. The drastic decrease of the grain boundary resistivity from 0.19 GΩ to  $\approx 6.5$  kΩ between 373 and 973 K is a consequence of an activation of defects, in first place oxygen vacancies located in the grain boundaries and generated during the mechanochemical treatment. A high amount of oxygen vacancies arises from the large density of the grain boundaries of nanocrystalline structures. It is a well known that the inherent feature of nanostructured materials is a significant fraction of atoms residing in the grain boundaries.<sup>35</sup> Therefore, it may be concluded that mechanochemical treatment, through the formation of significant defect structure(s), has an effect on the ionic conductivity.

TABLE I. Grain,  $R_g$ , and grain boundary,  $R_{gb}$ , resistivities, grain boundary capacitance,  $C_{gb}$ , specific resistivity,  $\rho$ , and specific conductivity,  $\sigma$ , at various temperatures of the pressed Bi<sub>0.78</sub>Hf<sub>0.59</sub>Zr<sub>0.63</sub>O<sub>3.61</sub> sample mechanochemically synthesized by 50 h of milling

Parameter	$t / ^\circ\text{C}$						
	100	200	300	400	500	600	700
$R_g / \text{k}\Omega$	25	24.5	23	22.5	$\approx 5$	$\approx 4$	$\approx 2$
$R_{gb} / \text{k}\Omega$	$0.19 \times 10^9$	$1.2 \times 10^6$	$21.1 \times 10^3$	$4.1 \times 10^2$	$\approx 1.4 \times 10^2$	$\approx 16$	$\approx 6.5$
$C_{gb} / \text{pF}$	13	25	25.5	31.8	$\approx 35$	$\approx 48$	–
$\rho / \Omega \text{ cm}$	$9.01 \times 10^8$	$5.99 \times 10^6$	$1.06 \times 10^5$	$2.02 \times 10^3$	$6.6 \times 10^2$	62	12.5
$\sigma / \text{S cm}^{-1}$	$1.11 \times 10^{-9}$	$1.67 \times 10^{-7}$	$9.43 \times 10^{-6}$	$4.94 \times 10^{-4}$	$1.52 \times 10^{-3}$	$1.62 \times 10^{-2}$	$8.00 \times 10^{-2}$

## CONCLUSIONS

A nanocrystalline  $\text{Bi}_{0.78}\text{Hf}_{0.59}\text{Zr}_{0.63}\text{O}_{3.61}$  solid solution with a fluorite-type  $\delta\text{-Bi}_2\text{O}_3$  structure was synthesized by prolonged mechanochemical treatment of a  $2\text{Bi}_2\text{O}_3 \cdot 3\text{HfO}_2$  powder mixture in a zirconia medium.

The reaction commenced at the very beginning of milling through the formation of a  $\beta\text{-Bi}_2\text{O}_3$  phase, which grew with the advancement of milling and was finely transformed to a single  $\delta\text{-Bi}_2\text{O}_3$  phase. The final phase transition was very likely assisted by the accumulation of  $\text{ZrO}_2$  arising from the milling tools. Thus, contamination of the milled materials, which in many situations must be judged as undesirable, presents here a favorable process.

According to DSC results, the  $\text{Bi}_{0.78}\text{Hf}_{0.59}\text{Zr}_{0.63}\text{O}_{3.61}$  solid solution was stable on heating and cooling between room temperature and  $900\text{ }^\circ\text{C}$ . This fact and the relatively high value of the electrical conductivity, close to  $0.1\text{ S cm}^{-1}$  for a temperature of  $700\text{ }^\circ\text{C}$ , make the mechanochemically synthesized  $\text{Bi}_{0.78}\text{Hf}_{0.59}\text{Zr}_{0.63}\text{O}_{3.61}$  solid solution a promising high oxide ion conductivity material.

*Acknowledgements.* This work was financially supported by the Ministry of Science and Technological Development of the Republic of Serbia (Grants No. 142030 and 141027).

## ИЗВОД

МЕХАНОХЕМИЈСКА СИНТЕЗА И ЕЛЕКТРИЧНА ПРОВОДНОСТ НАНОКРИСТАЛНОГ  $\delta\text{-Bi}_2\text{O}_3$  СТАБИЛИСАНОГ СА  $\text{HfO}_2$  И  $\text{ZrO}_2$ 

МИОДРАГ ЗДУЈИЋ<sup>1</sup>, ДЕЈАН ПОЛЕТИЋ<sup>2</sup>, ЧЕДОМИР ЈОВАЛЕКИЋ<sup>3</sup> И ЉИЉАНА КАРАНОВИЋ<sup>4</sup>

<sup>1</sup>Институт за техничке науке САНУ, Кнез Михаилова 35, Београд, <sup>2</sup>Капедра за општу и неорганску хемију, Технолошко–металуршки факултет, Универзитет у Београду, Карнегијева 4, Београд, <sup>3</sup>Институт за мултидисциплинарна истраживања, Кнеза Вишеслава 1а, Београд и <sup>4</sup>Лабораторија за кристалографију, Рударско–геолошки факултет, Универзитет у Београду, Београд

Смеша прахова  $\alpha\text{-Bi}_2\text{O}_3$  и  $\text{HfO}_2$  у моларном односу 2:3 механохемијски је третирана у планетарном млину у атмосфери ваздуха, користећи цирконијумске посуде и куглице као медијум за млевење. После 50 h млевења, механохемијска реакција доводи до стварања нанокристалне  $\delta\text{-Bi}_2\text{O}_3$  фазе (чврсти раствор флуоритске структуре  $\text{Bi}_{0.78}\text{Hf}_{0.59}\text{Zr}_{0.63}\text{O}_{3.61}$ ), величине кристалита 20 nm. Механохемијска реакција отпочиње у самом почетку млевења и праћена је акумулацијом  $\text{ZrO}_2$  који потиче од медијума за млевење. Узорци добијени после различитих времена млевења карактерисани су рендгенском структурном и термијском анализом. Електрична својства млевених и пресованих  $\text{Bi}_{0.78}\text{Hf}_{0.59}\text{Zr}_{0.63}\text{O}_{3.61}$  прахова испитивана су импедансном спектроскопијом у температурном опсегу од 100 до  $700\text{ }^\circ\text{C}$ . Добијена електрична проводност је  $9,43 \cdot 10^{-6}$  и  $0,080\text{ S cm}^{-1}$  за температуру 300 и  $700\text{ }^\circ\text{C}$ , редом.

(Примљено 13. маја, ревидирано 22. јуна 2009)

## REFERENCES

1. H. Ishiwara, M. Okuyama, Y. Arimoto, Eds., *Ferroelectric Random Access Memories – Fundamentals and Applications* (Topics in Applied Physics, Vol. 93), Springer-Verlag, Berlin, 2004

2. A. R. West, *Basic Solid State Chemistry*, 2<sup>nd</sup> ed., Wiley, Chichester, 2004, p. 345
3. P. Shuk, H. -D. Wiemhofer, U. Guth, W. Gopel, M. Greenblatt, *Solid State Ionics* **89** (1996) 179
4. J. C. Boivin, G. Mairesse, *Chem. Mater.* **10** (1998) 2870
5. E. M. Levin, R. S. Roth, *J. Res. Natl. Bur. Stand.* **68A** (1964) 189
6. H. A. Harwig, *Z. Anorg. Allg. Chem.* **444** (1978) 151
7. N. Cornei, N. Tancret, F. Abraham, O. Mentré, *Inorg. Chem.* **45** (2006) 4886
8. A. Helfen, S. Merkourakis, G. Wang, M. G. Walls, E. Roy, K. Yu-Zhang, Y. Leprince-Wang, *Solid State Ionics* **176** (2005) 629
9. G. Gattow, H. Schröder, *Z. Anorg. Allg. Chem.* **318** (1962) 176
10. S. Kashida, K. Nakamura, *Philos. Mag. Lett.* **73** (1996) 279
11. U. Pirnat, M. Valant, B. Jančar, D. Suvorov, *Chem. Mater.* **17** (2005) 5155
12. M. Valant, B. Jančar, U. Pirnat, D. Suvorov, *J. Eur. Ceram. Soc.* **25** (2005) 2829
13. M. Yashima, D. Ishimura, *Chem. Phys. Lett.* **378** (2003) 395
14. C. D. Ling, M. Johnson, *J. Solid State Chem.* **177** (2004) 1838
15. N. Portefaix, P. Conflant, J. C. Boivin, J. P. Wignacourt, M. Drache, *J. Solid State Chem.* **134** (1997) 219
16. F. Krok, I. Abrahams, W. Wrobel, S. C. M. Chan, A. Kozanecka, T. Ossowski, J. R. Dygas, *Solid State Ionics* **175** (2004) 335
17. O. Labidi, M. Drache, P. Roussel, J. P. Wignacourt, *Solid State Sci.* **10** (2008) 1074
18. D. Poleti, Lj. Karanović, M. Zdujić, Č. Jovalekić, Z. Branković, *Solid State Sci.* **6** (2004) 239
19. M. Zdujić, D. Poleti, Č. Jovalekić, Lj. Karanović, *J. Non-Cryst. Solids* **352** (2006) 3058
20. Č. Jovalekić, M. Zdujić, D. Poleti, Lj. Karanović, M. Mitrić, *J. Solid State Chem.* **181** (2008) 1321
21. W. Kraus, G. Nolze, *PowderCell for Windows*, V.2.4, Federal Institute for Materials Research and Testing, Berlin, Germany, 2000.
22. R. G. Garwey, *Powder Diff.* **1** (1986) 114
23. H. P. Klug, L. E. Alexander, *X-Ray Diffraction Procedures*, 2<sup>nd</sup> ed., Wiley, New York, 1974, p. 687
24. I. Abrahams, A. J. Bush, S. C. M. Chan, F. Krok, W. Wrobel, *J. Mater. Chem.* **11** (2001) 1715
25. S. L. Sorokina, A. W. Sleight, *Mater. Res. Bull.* **33** (1998) 1077
26. A. Ayala, A. López-García, A. G. Leyva, M. A. R. De Benyacar, *Solid State Commun.* **99** (1996) 451
27. L. Passerini, *Gazz. Chim. Ital.* **60** (1930) 762
28. *Impedance Spectroscopy: Emphasizing Solid Materials and Systems*, J. R. MacDonald, Ed., Wiley, New York, 1987, p. 33
29. N. A. S. Webster, C. D. Ling, C. L. Raston, F. J. Lincoln, *Solid State Ionics* **178** (2007) 1451
30. A. Watanabe, *Solid State Ionics* **96** (1997) 75
31. C. K. Lee, C. S. Lee, A. Watanabe, D. C. Sinclair, *Solid State Ionics* **171** (2004) 237
32. V. I. Smirnov, V. G. Ponomareva, Yu. M. Yukhin, N. F. Uvarov, *Solid State Ionics* **156** (2003) 79
33. O. Labidi, P. Roussel, M. Huve, M. Drache, P. Conflant, J. P. Wignacourt, *J. Solid State Chem.* **178** (2005) 2247
34. Z. S. Macedo, C. R. Ferrari, A. C. Hernandez, *J. Eur. Ceram. Soc.* **24** (2004) 2567
35. E. Gaffet, G. Le Caër, in *Encyclopedia of Nanoscience and Nanotechnology*, Vol. 10, H. S. Nalwa, Ed., American Scientific Publishers: Stevenson Ranch, California, 2004, pp. 1–39.